

## Calibration of Underwater Polarization Image Based on the Radian of Distorted Curves in the Checkboard

Jiaming Wei, Qi Li and Lili Zhang<sup>1\*</sup>

<sup>1</sup>College of Computer and Information Engineering, Hohai University, Nanjing, 210098, China

<sup>1</sup>[lilzhang@hhu.edu.cn](mailto:lilzhang@hhu.edu.cn)

### Abstract

*The calibration of polarization imaging system is the premise to obtain target polarization information accurately, in this paper, we propose a method of calibration based on the radian of distorted curves in the checkboard to solve the problem of losing polarization information in the underwater distorted polarization images. Firstly, we use the radian of distorted curves in the checkboard to calculate the coordinates of distortion center, and calibrate the region near the distortion center. Then we use the calibrated region to reconstruct the whole image. Finally, we combine the distorted image, the reconstructed image and the distortion model to obtain the calibration parameters. With these parameters we can get the calibrated polarization images. The experiments show that our method can calibrate the polarization image accurately, reduce the coupled error and calculate parameters independently.*

**Keywords:** Polarization imaging system; Calibration; Radian of distorted curve; Distortion model

### 1. Introduction

In recent years, with the development of polarization optics, the polarization imaging are applied widely [1-4]. However, it has non-linear geometric distortion like the other optical imaging systems due to the surface curvature of the lens, the dislocation between the lens center and the imaging plane, so there are still different distortion such as radial distortion, tangential distortion, and thin prism distortion in the polarization imaging system. The problem will be more serious when the waterproof cover or wide-angle lens is installed on the underwater monitoring devices.

The main method to solve the problem of distortion is to obtain system's calibration parameters through calibration methods, then use these parameters to calibrate distorted image. Currently, the calibration methods of the optical imaging system include TSAI [5] method, ZZY [6] method and so on. TSAI calibration algorithm is a two-step calibration method, according to internal intrinsic parameters of camera and mapping relationship between real scene and image to obtain internal and external unknown parameters of the camera. When use Tsai method to calculate the parameters, we obtain the internal and external parameters separately. TSAI used the radial constraint to calculate the external parameters of the camera such as translation matrix, rotation matrix and rotation angle, then got the initial values for iteration of calibration based on the pinhole model, and got the camera calibration parameters through nonlinear optimization search such as distortion parameters and focal length ratio. TSAI has higher calibration accuracy, but we need obtain the three-dimensional calibration points of the calibration block on the different planes, which will be restricted by the calibration block's accuracy. In addition, TSAI put the image center as the distortion center which makes the ratio of calibrated

---

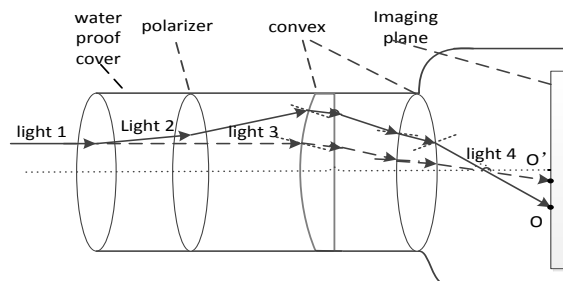
\*Corresponding Author

image being inconsistent with the ideal image. ZZY is a camera calibration method between traditional method of calibration and self-calibration method of calibration, it just requires a camera to take multiple pictures of calibration plate from different directions, through correspondence between each feature point on calibration board and image point of plane, which is the homography of each image for camera calibration. He converted the three-dimensional coordinates calculation into two-dimensional coordinates calculation, and got the camera calibration parameters through pinhole model, finally got the camera calibration parameters based on the maximum likelihood method [7] through nonlinear operation. ZZY calibration method makes it more practical to use plane calibration checkboard instead of the calibration block, but its parameter solution process is not independent which can make large coupling error. Recently, researchers proposed some improved methods based on the above two methods. Xu proposed one rectangular geometric camera calibration method [8], according to the cross-ratio relationships of projective geometry and the character of harmonic conjugate, using the vanishing points to calculate calibration parameters linearly instead of the maximum likelihood method of nonlinear operation; Rahman [9] proposed an efficient method for wide-angle lens distortion calibration, which use the combination of the pinhole model and lens distortion model instead of holography matrix equation to calculate the distorted center, and then used nonlinear iterative method to get calibration parameters. In addition, Melo [10] proposed a new real-time calibration method, to detect the edge for single calibration image and compute these control points within the region by nonlinear iterative method based on the pinhole model. However, these methods still have big coupling error in the process of calculating calibration parameters.

In this paper, we will propose a method of calibration based on the radian of distorted curves in the checkboard which can be applied in the underwater monitoring. Firstly, we use the radian of distorted curves in the checkboard to calculate coordinates of distortion center, and calibrate the region near the distortion center. Then we use the calibrated region to reconstruct the whole image. Finally, we combine the distorted image, the reconstructed image and the distortion model to obtain the calibration parameters. The experiments show that our method can calibrate the polarization image accurately, reduce the coupled error and calculate parameters independently.

## 2. Related Work

Underwater polarization imaging system is composed of the optical imaging system, polarizer and glass waterproof cover. Since the surface of the polarizer and the waterproof cover are not completely smooth and exist convex surface, so underwater polarization imaging model needs to consider the distortion caused by the polarizer and glass. Lens distortion of underwater polarization imaging system is shown in Figure 1.



**Figure 1. Lens Distortion of Underwater Polarization Imaging System**

As we know, the underwater incident light is composed of scattered light and refracting light, and in fact the waterproof cover exists convex surface. Therefore the imaging point

O' deviates from the ideal point O. Due to light 1 occurs offsets in the radial and tangential when it passes through a waterproof cover vertically because of the refraction. Refracted light 2 passes through the polarizer which surface is not smooth at some angle, so the refracted light 3 through the polarizer and light 2 are not parallel, and occurs offset in the radial and the tangential direction. Point O' on the imaging plane is the imaging point when the light does not pass through waterproof cover or polarizer which is dotted line. Non-smooth of waterproof cover, polarizer and convex led to the radial distortion and tangential distortion of the imaging system.

In order to improve the accuracy of radial calibration, we use the distortion model of optical imaging system to get the calibration parameters, and extend the coefficient of radial distortion to three-dimension. We also consider the effect of tangential distortion. The relationship between the distortion point and the ideal point is shown in Figure 2, where  $(X_d, Y_d)$  is the point coordinates in distorted image, and  $(X_p, Y_p)$  is the point coordinates in calibrated image.

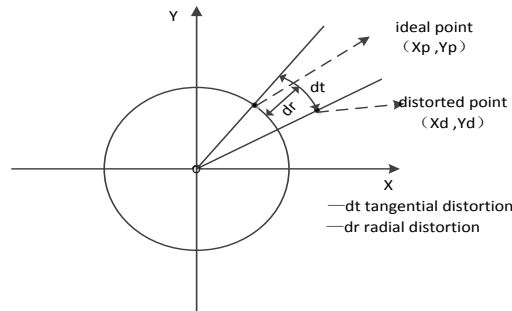


**Figure 2. Relationship between Distortion Point and Ideal Points**

Let distorted point be  $q_d = (X_d, Y_d)$  and ideal point be  $q_p = (X_p, Y_p)$ , and the distortion model defines the mapping from  $q_d$  to  $q_p$ . The mapping described [11] as the Formula (1):

$$\begin{cases} X_d = X_p + X_p(k_1 r^2 + k_2 r^4 + k_3 r^6) + p_1(2X_p^2 + r^2) + 2p_2 X_p Y_p \\ Y_d = Y_p + Y_p(k_1 r^2 + k_2 r^4 + k_3 r^6) + 2p_1 X_p Y_p + p_2(2Y_p^2 + r^2) \end{cases} \quad (1)$$

Where  $r$  represents the distance from the distortion center to the ideal point,  $k$  represents the parameter of radial distortion,  $p$  represents the parameter of tangential distortion and  $r = \sqrt{(X_p - U)^2 + (Y_p - V)^2}$ ,  $(U, V)$  is the distortion center coordinate.

### 3. Calibration

Lens distortion can cause the straight line being curve in calibration checkboard of the imaging plane, and also lens distortion is proportional to the projected curve radian. We use the minimum curve radian of distorted curves to obtain no-distortion straight line by iterative fitting, and obtain the distortion center and reduce the computing error of distortion center. Then, based on the sub regional strategy, we put the region near the distortion center as the basis of the image reconstruction and replace the error of whole image reconstruction by correction error of the local region, as a result, we can reduce the error of corrected image.

Our method consists of three components. Firstly, we use the least squares method [12] to fit the best optical center line and calculate the distortion center coordinates based on the radian of distorted curves. Secondly, we select the neighborhood region of the distortion center as the initial calibration region, and put the line in the calibrated initial region as the baseline to continue the whole image reconstruction. Lastly, based on the

lens distortion model, we substitute the coordinates corresponding to the point before and after calibrating into the mapping relationship to obtain the calibration parameters.

### 3.1. Distortion Center

**3.1.1. Radian Calculation:** Radian of distortion curve is the radian of the line in the checkboard of the distorted image and is proportional to the fitting error which can be obtained through fitting the points on the same curve:

$$r_i = k \sum_{k=1}^j (y_{i,k} - a_i x_{i,k} - b_i)^2 (k > 0) \quad (2)$$

Where  $r_i$  represents the curve radian,  $(y_{i,k}, x_{i,k})$  is the coordinate of the k-th point on the i-th curve and  $a_i, b_i$  represent the parameters of the fitting line.

We can calculate the radian of all curves in Figure 3, based on the Formula (2). Due to bending direction of the curves distributed on two sides of distorted center is opposite, we choose two curves with the smallest radian from X-axis and Y-axis direction respectively, and denote them as L1, L2 and L3, L4, respectively.

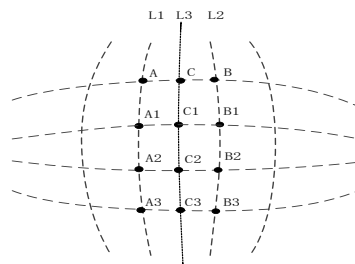


**Figure 3. Optical Center Line**

**3.1.2. Calculation of Distortion Center:** As shown in Figure 3, the radian of curve L1 and curve L2 are minimum, and point A being on the curve L1 and point B being on the curve L2. We can use the Formula (3) to calculate the coordinate of intermediate point C.

$$\begin{cases} x_{3,k} = x_{1,k} + (x_{2,k} - x_{1,k}) \frac{\max\{r_1, r_2\}}{r_1 + r_2} \\ y_{3,k} = y_{1,k} + (y_{2,k} - y_{1,k}) \frac{\max\{r_1, r_2\}}{r_1 + r_2} \end{cases} \quad (3)$$

Where  $(x_{1,k}, y_{1,k}), (x_{2,k}, y_{2,k}),$  and  $(x_{3,k}, y_{3,k})$  are the coordinates of the k-th point on curve L1, curve L2 and fitted curve, respectively.

Calculating the intermediate point coordinates of each line, and then we link all the intermediate points to get curve L3, and calculate the radian  $r_3$ . If  $r_3 < r_1$ , curve L3 will be denoted as curve L1 and  $r_3$  will be denoted as  $r_1$ . Otherwise, if  $r_3 < r_2$ , curve L3 will be denoted as curve L2 and  $r_3$  will be denoted as  $r_2$ . Keeping on this process with the smallest radian until  $|r_3| < \varepsilon$ , let  $\varepsilon$  be 0.001 in this paper. Finally, L3 is the optical center line Ly of the Y-axis. Similarly, we can get the optical center line Lx of the X-axis.

With the two expressions of optical center line, we can get the Formula (4), which can be used to calculate the coordinate of distortion center.

$$\begin{cases} y_1 = a_1 x_1 + b_1 \\ y_2 = a_2 x_2 + b_2 \end{cases} \quad (4)$$

Where  $x_1, y_1$  represent the optical center line Lx,  $a_1, b_1$  represent the parameters of the line, and  $x_2, y_2$  represent the optical center line Ly,  $a_1, b_1$  represent the parameters of the line.

Changing the form of the Formula (4), we can obtain the distortion center (U, V), which is shown as Formula (5).

$$\begin{bmatrix} U \\ V \end{bmatrix} = \begin{bmatrix} 1 & -a_1 \\ 1 & -a_2 \end{bmatrix}^{-1} \begin{bmatrix} b_1 \\ b_2 \end{bmatrix} \quad (5)$$

### 3.2. Reconstruction

**3.2.1. Analysis of Character:** Due to the degree of distortion near the neighborhood of the distortion center is smaller [13], and the calibration error which uses distortion central region as the initial region to calibrate is smaller than that uses calibration checkboard to continue the whole image calibration, so in this paper, we choose the regions with size 3\*3 in Figure 4. The chosen initial region contains 17 points, denoted as  $q_1(x_i, y_j), q_2(x_i, y_{j+1}), q_3(x_i, y_{j+2}), q_4(x_i, y_{j+3}), q_5(x_{i+1}, y_j), q_6(x_{i+1}, y_{j+1}), q_7(x_{i+1}, y_{j+2}), q_8(x_{i+1}, y_{j+3}), q_9(x_{i+2}, y_j), q_{10}(x_{i+2}, y_{j+1}), q_{11}(x_{i+2}, y_{j+2}), q_{12}(x_{i+2}, y_{j+3}), q_{13}(x_{i+3}, y_j), q_{14}(x_{i+3}, y_{j+1}), q_{15}(x_{i+3}, y_{j+2}), q_{16}(x_{i+3}, y_{j+3})$ , and  $O(U, V)$ , respectively.

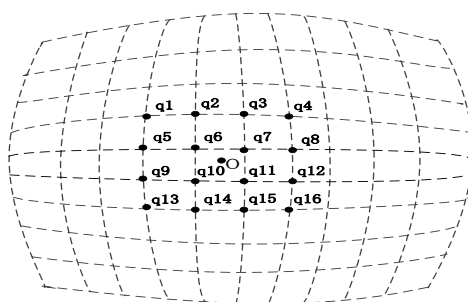


Figure 4. Initial Calibration Domain

#### 1) Straight line

All points on the same direction of the ideal checkboard must be a straight line. If the point  $q_{i,j} = (x_i, y_j)$  is on the line L, there must be one linear equation satisfying  $y_i = a_1 x_i + b_1$ , and the coefficients  $a_1$  and  $b_1$  can be obtained by the four points on the straight line by fitting. We use the fitting error  $\delta_i$  to measure the calibration, where

$$\delta_i = \sum_j (y_i - a_1 x_i - b_1)^2 \quad (6)$$

The smaller  $\delta_i$  is, the straight line which contains calibrated points is closer to the ideal no-distortion line. Therefore, we use Formula (7), to make the calibrated points meeting the character.

$$p_1 = \sum_{l=1}^4 \sum_{i=1}^4 (y_i - a_l x_i - b_l)^2 \quad (7)$$

The calibration checkboard in the paper is  $m * n$ , so these points on the same column also meet the formula (8).

$$p_2 = \sum_{r=1}^4 \sum_{i=1}^4 (y_i - a_r x_i - b_r)^2 \quad (8)$$

## 2) Equal distance

Distance of any two adjacent points in vertical and horizontal direction of the ideal checkboard must be equal. If the point  $q_{i,j} = (x_i, y_j)$  is on the line L, then denote the two points in mutually perpendicular directions by  $q_{i+1}(x_{i+1}, y_{i+1})$  and  $q_{i+4}(x_{i+4}, y_{i+4})$ . If there is not any distortion, the length of square cell edge is equal in the checkboard which is C, so it must meet the Formula (9).

$$\sqrt{(x_i - x_{i+1})^2 + (y_i - y_{i+1})^2} = \sqrt{(x_i - x_{i+4})^2 + (y_i - y_{i+4})^2} = C \quad (9)$$

If there has distortion, the relationship between any two adjacent points in the image cannot satisfy the Formula (9). And we use the Formula (10) to make the calibrated points meet the Formula (9).

$$p_3 = \sum_{r=1}^3 \sum_{i=1}^3 \sqrt{(x_{r+i} - x_{r+i+1})^2 + (y_{r+i} - y_{r+i+1})^2} + \sqrt{(x_{(r+1)i} - x_{(r+1)i+1})^2 + (y_{(r+1)i} - y_{(r+1)i+1})^2} - 2C \quad (10)$$

When using the formula (10), we reduce the initial region size to  $2*2$  in order to avoid the phenomenon of subscript out of bounds.

## 3) Perpendicular

Any line in the vertical direction is perpendicular to any line in the horizontal direction of the ideal checkboard. When calibrated images meet above two characters, the cell in calibrated image is square or diamond. So we need to use the Formula (11) to make the lines in X-axis and Y-axis being mutually perpendicular.

$$p_4 = \sum_{r=1}^4 \sum_{l=1}^4 (a_l a_r + 1)^2 \quad (11)$$

Where  $a_l$  and  $a_r$  represent the slope of the horizontal line and vertical line.

**3.2.2. Region Calibration:** In order to minimize the calibration error, we use all constraint equations from Formula (7) to Formula (11) to obtain the Formula (12).

$$P = p_1 + p_2 + p_3 + p_4 \quad (12)$$

The length of the checkboard square cell is defined as Lcm, the set  $q_i$  of the distorted point coordinates and the parameters  $(a, b)$  of initial line is the inputs of the LM iterative algorithm [14] to make the coordinate  $q_{i,d}$  closer to ideal coordinate  $q_{i,p}$  and the calibrated line closer to the ideal no-distortion line until the distance between adjacent points infinitely close to L, then we can achieve the calibrated initial region.

**3.2.3. Image Reconstruction:** We make use of the calibrated initial region and three characters which are introduced in section 3.2.1 to reconstruct image based on the eight calibrated lines of the initial region, then we can get the reconstructed image which is calibrated image.

The process in detail as follows.

Step 1: Put the eight straight lines in  $X, Y$  axis direction as the baselines in the initial region, use the character of equal distance to get the rest  $n-4$  points in  $X$  direction and the rest  $m-4$  points in  $Y$  direction.

Step 2: In the left and right sides of the initial region, use 4 points in  $Y$  direction to fit a straight line for the rest  $n-4$  columns.

Step 3: In the upper and lower sides of the initial region, use 4 points in  $X$  direction to fit a straight line for the rest  $m-4$  columns.

Step 4: Calculate the crossing points of all straight lines which are the calibrated points.

### 3.3. Calibration Parameters

Based on the distortion model in Formula (1), we calculate the distortion parameters  $k_1, k_2, k_3, p_1,$  and  $p_2$  of the polarization imaging system. We can get the Formula (13) from the Formula (1):

$$\begin{bmatrix} X_p r^2 & X_p r^4 & X_p r^6 & 2X_p^2 + r^2 & 2X_p Y_p \\ Y_p r^2 & Y_p r^4 & Y_p r^6 & 2X_p Y_p & 2Y_p^2 + r^2 \end{bmatrix} \begin{bmatrix} k_1 \\ k_2 \\ k_3 \\ p_1 \\ p_2 \end{bmatrix} = \begin{bmatrix} X_d - X_p \\ Y_d - Y_p \end{bmatrix} \quad (13)$$

Where  $r = \sqrt{(X_p - U)^2 + (Y_p - V)^2}$ .

Using the Formula (13),  $m$  distorted points and  $m$  calibrated points, we can get an equation set with  $2*m$  equations which can be simply denoted by Formula (14), and we can get the distortion parameters  $k_1, k_2, k_3, p_1,$  and  $p_2$  from Formula(14) by the least squares method.

$$UK = D \quad (14)$$

Where  $K = [k_1, k_2, k_3, p_1, p_2]^T$ .

## 4. Experiments

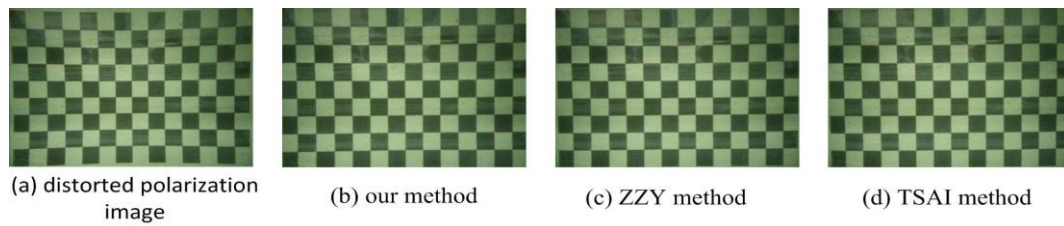
The resolution of CMOS camera is  $1024 \times 1024$  in imaging system. Polarizer is MASSA 460mmPL. Calibration checkboard is  $420mm \times 270mm$  and the size of the square cell is  $30mm \times 30mm$ .

### 4.1. Calibration Experiment of Underwater

#### 1) Calibration of calibration checkboard

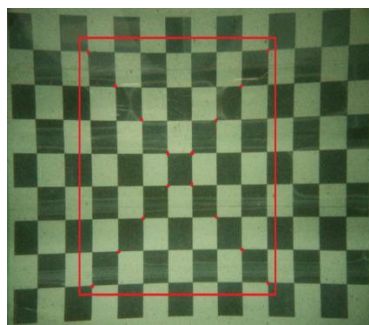
As shown in Figure 5, we firstly get the underwater distorted polarization image of the calibration checkboard, and then use our method, ZZY method and TSAI method respectively. Figure 5(a) is the distorted polarization image, Figure 5(b), Figure 5 (c) and

Figure 5 (d) are the calibrated images gotten by our method, ZZY method, and TSAI method, respectively.



**Figure 5. Calibrated Images Gotten by Different Methods**

As shown in Figure 6, we test the results of the points in the red box in the diagonal before and after calibrating. And Figure 7, shows the change of different calibration methods before and after calibrating.



**Figure 6. Region of Comparison**

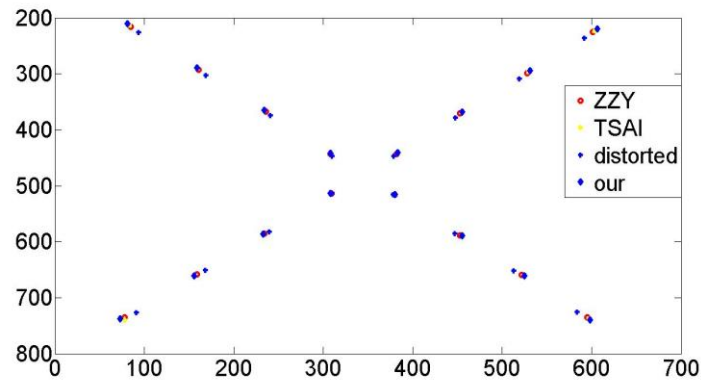


**Figure 7. Comparison of Test Point Coordinates**

In Figure 7, blue diamond symbol, red circle symbol, yellow asterisks symbol and blue plus symbol represent our method calibrated points, ZZY method calibrated points, TSAI method calibrated points and distorted points, respectively. As shown in Figure 7, the points of our method space equidistantly in the diagonal, but ZZY and TSAI are not.

In the paper, we use the fitting error and average pixel error as the metrics of calibration. The formulas of fitting error and average pixel error are as below:

$$\begin{cases} \delta_i = \sum_j (y_{i,j} - a_i x_{i,j} - b_i)^2 \\ \delta_j = \sum_i (y_{i,j} - a_j x_{i,j} - b_j)^2 \end{cases} \quad (15)$$



$$err = \frac{\sum_{j=1}^{13} \delta_j}{n} + \frac{\sum_{i=1}^8 \delta_i}{m} \quad (16)$$

In above two formulas,  $\delta_i$  is the fitting error of line,  $\delta_j$  is the fitting error of column, m is the number of the lines, n is the number of columns, subscript X represents X-axis, and Y represents Y-axis. Figure 8, is the performance of different calibration methods for the distorted calibration checkboard. The value of line of vertical axis represents the numbers of line in the checkboard from 1 to 13, every line have 8 points. The value of line of horizontal axis represents the numbers of column in the checkboard from 1 to 8, every column have 13 points. The value of Y-axis represents fitting error, the smaller it is, the better the calibration effect is.

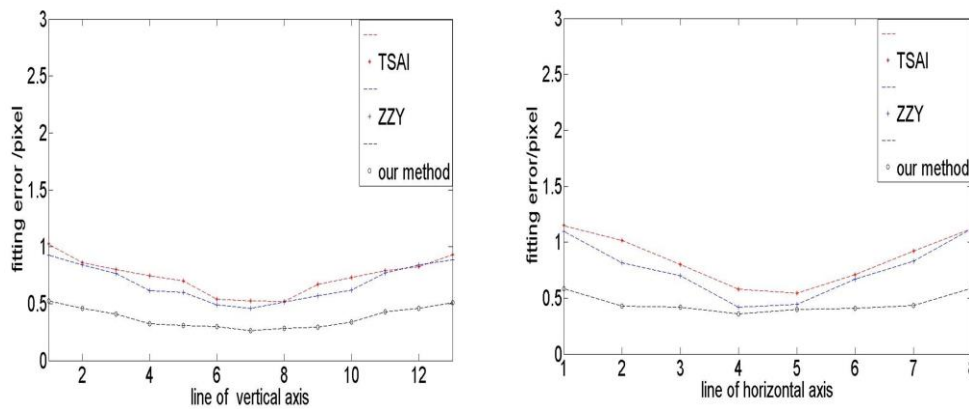


**Figure 8. Fitting Error of Calibrated Checkboard**

**Table 1. Average Pixel Error of Three Methods**

	average pixel error /pixel on X -axis	average pixel error /pixel on Y-axis
Our method	0.3767	0.4521
ZZY method	0.7423	0.8979
TSAI method	0.6838	0.7622

Compare the three sets of experimental data of average pixel error in Table 1, we can find that the average pixel error of our method reduces significantly, so our method is better.

2) Calibration of target

Considering the different degrees of distortion in the different optical environment, we choose two underwater scenes, one is in the sink in laboratory and the other is in the Donghu lake in our school.

In Figure 9, the original distorted polarization image is taken in the sink with adequate light and a small water turbidity, the reference target is a metal straight bar, and the acquired reference target image is relatively clear and high contrast. Figure 9 (a)-(c), represent distorted polarization image of 0 degree, 45 degree and 90 degree respectively.

Figure 10, is the calibrated polarization image after using different calibration methods, Figure 10(a1)-(a3), represent calibrated polarization image of 0 degree by ZZY method, TSAI method and our method respectively, Figure 10(b1)-(b3), represent calibrated polarization image of 45 degree by ZZY method, TSAI method and our method respectively, Figure 10(c1)-(c3), represent calibrated polarization image of 90 degree by ZZY method, TSAI method and our method respectively.

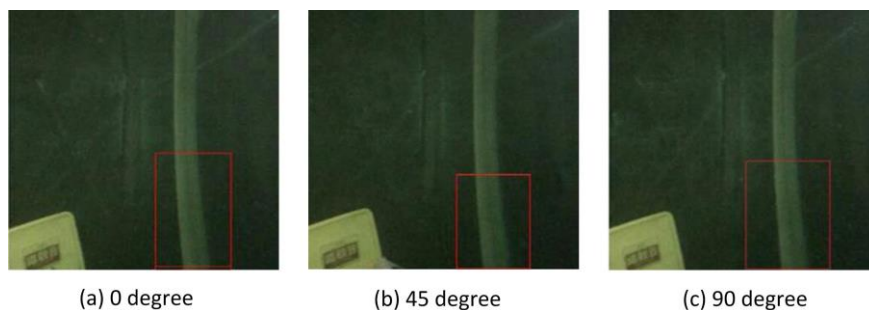


**Figure 9. Original Distorted Polarization Images in the Sink**

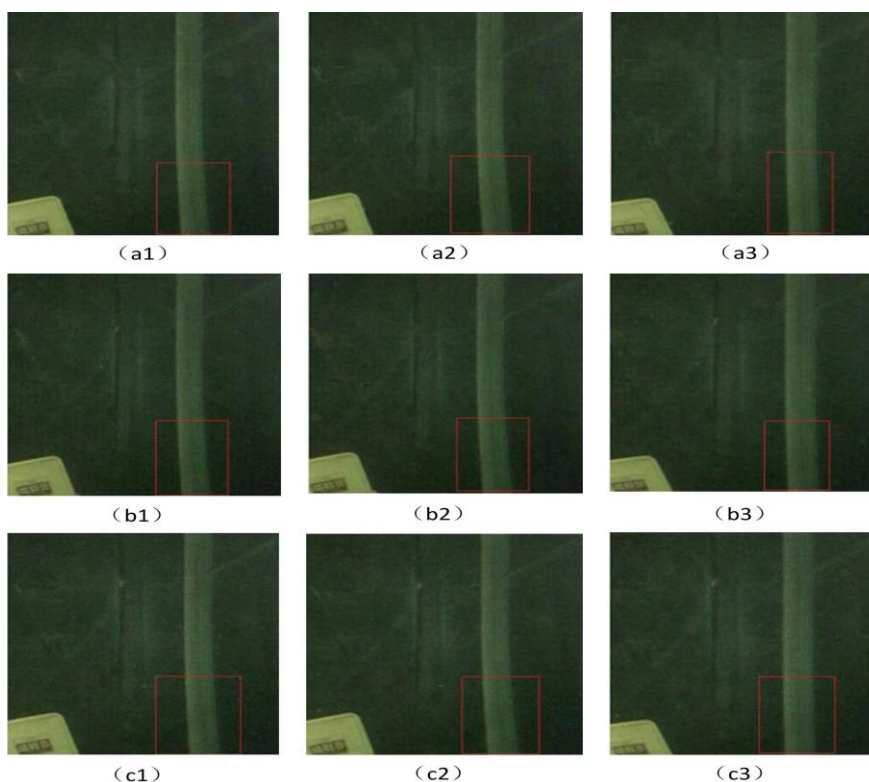


**Figure 10. Calibrated Images of Distorted Polarization Images in the Sink**

As shown in Figure 9, the straight bar in the red box of Figure 9(a), is obviously curved. Comparing three calibrated polarization images in any line of Figure 10, the two former images' degree of the curve in red box relative to distorted image is smaller and the bar is nearly straight in the red box which is calibrated by our method.

In Figure 9, the original distorted polarization image is taken in the Donghu lake which has low light and a big water turbidity, the reference target is a rectangular plate, and the acquired reference target image is relatively vague and low contrast. Figure 9(a)-(c), represent distorted polarization image of 0 degree, 45 degree and 90 degree respectively. Figure 10, is calibrated polarization image after using different calibration methods,

Figure 10(a1)-(a3), represent calibrated polarization image of 0 degree by ZZY method, TSAI method and our method respectively, Figure 10 (b1)-(b3), represent calibrated 45 degree polarization image of ZZY method ,TSAI method and our method respectively, Figure 10(c1)-(c3), represent calibrated 90 degree polarization image of ZZY method, TSAI method and our method respectively.

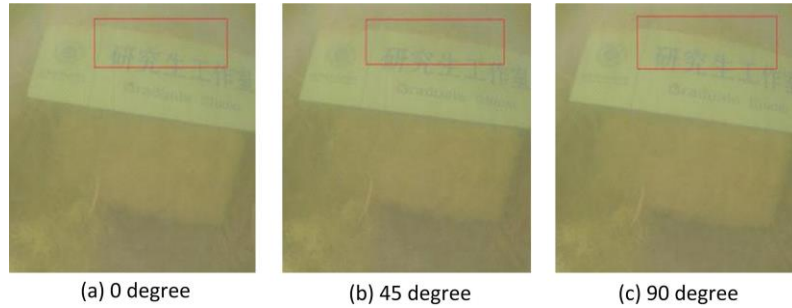


**Figure 11. Original Distorted Polarization Images in Donghu Lake**

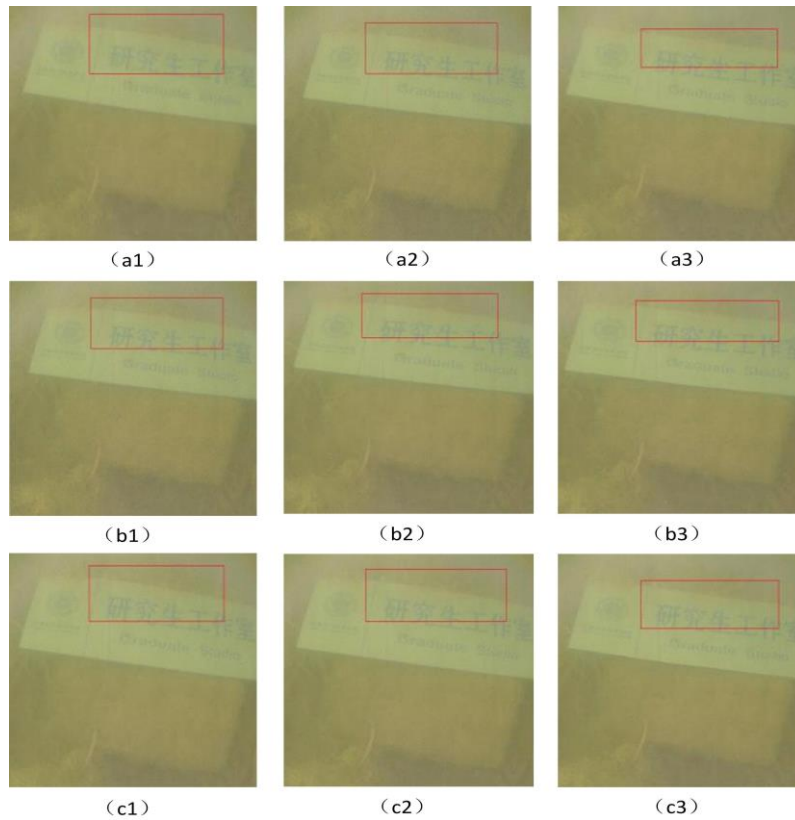


**Figure 12. Calibrated Images of Distorted Polarization Images in Donghu Lake**

From Figure 11, we can see that the edge of the plate in the red box is obviously curved. Comparing three calibrated polarization images in any line of Figure 12, such as (b1)-(b3), the calibrated image obtained by our method is better than obtained by ZZY method or TSAI method, since our method calculates the distortion center and calibration parameters independently, so we can avoid the coupling error. We adopt method of radian of distorted curves to correct the coordinates error which caused by water refraction. These make our method better than other two methods in underwater scene.

We use matlab to extract the time of distortion parameters computation for the above-mentioned three methods, and Table 2, gives the running time of the three methods, and our method costs the minimum time. The computer of the experiment is configured with i7-2600 processor, clocked at 3.4GHz, memory 4GB, Windows7X64 Professional Edition operating system and matlab version is R2009a.

**Table 2. The Comparison of Three Methods on Operation Time**

Algorithm	our method	ZZY	TSAI
running time/s	5.12	13.26	14.61

#### 4.2. Comparison of the Calibrated Image Polarization Information

In order to verify the calibration efficiency of the acquired target edge contour information after applying our method. We use ZZY, TSAI and our method to achieve the polarization angle (AOP) images based on the Stokes [15] which are shown in Figure 13.

Figure 13(a)-(c), represent distorted polarization image of 0 degree, 45 degree and 90 degree respectively and Figure 13(d)-(g), represent polarization angle images of non-calibration, ZZY method, TSAI method and our method, respectively.

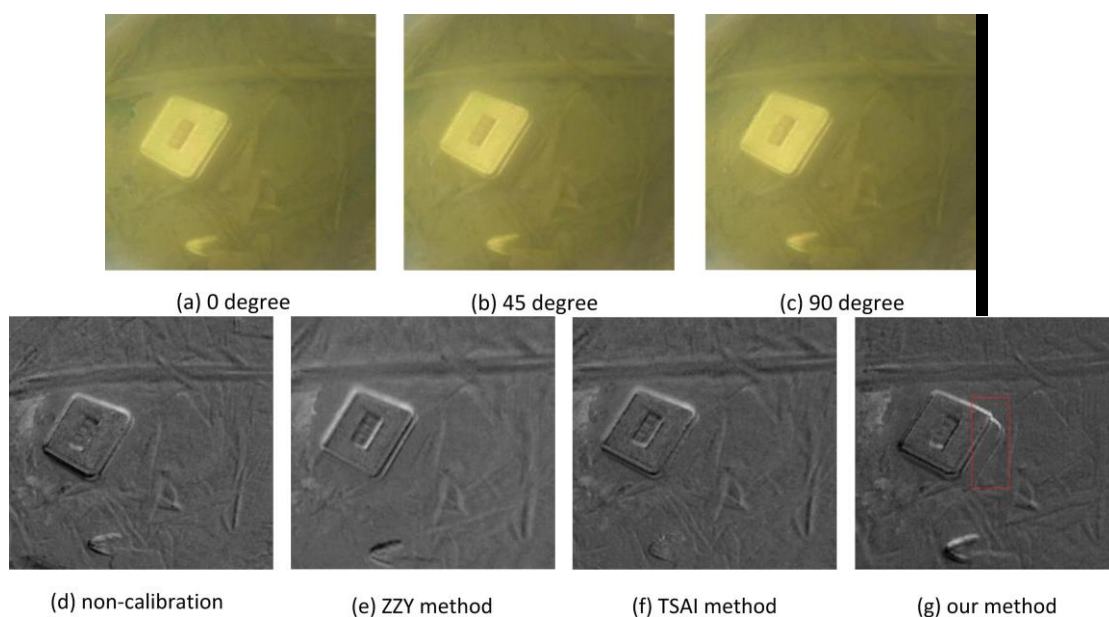


**Figure 13. Comparison of AOP By Different Methods**

In Figure 13, we choose the tin as the target, then compare the effect of AOP by different calibration methods. Comparing the Figure 13(d), and Figure 13(e), the edge of the tin in the bottom and in the middle shows vague in Figure 13(d), and the edge of the tin in the bottom and in the middle shows more clearly, the edge of the tin in the right shows partial in Figure 13(e); Comparing the Figure 13(d), and Figure 13(f), the edge of the tin in the left shows two layer edge clearly than Figure 13(e); Comparing the Figure 13(d) and Figure 13(g), the edge of the tin shows clearly in Figure 13(d), and the edge of right bottom shows clearly in Figure 13(g). We can find that the edge in the red frame in Figure 13(g), is the most clearly among all the AOP images. So we can get more texture information by applying our method to calibrate the distorted polarization image.

The comparison of the AOP images obtained from different calibration methods is shown in Figure 14. Entropy can reflect the aggregation feature of the image's intensity

distribution and reflects the image edge information effectively. If the entropy is larger, the image edge contains more information and the effect of contours show is better. Otherwise, if the entropy is smaller, the image edge contains less information. And the average gradient reflects the contrast of image detail and texture transform features of the image edge. If the gradient is larger, the image contains more levels and more clearly. Standard deviation reflects the image contrast between target and background. The bigger contrast causes the better visual effects.

In Figure 14, the X-axis from left to right are non-calibration, ZZY method, TSAI method and our method respectively, and the Y-axis represents the value of corresponding index.

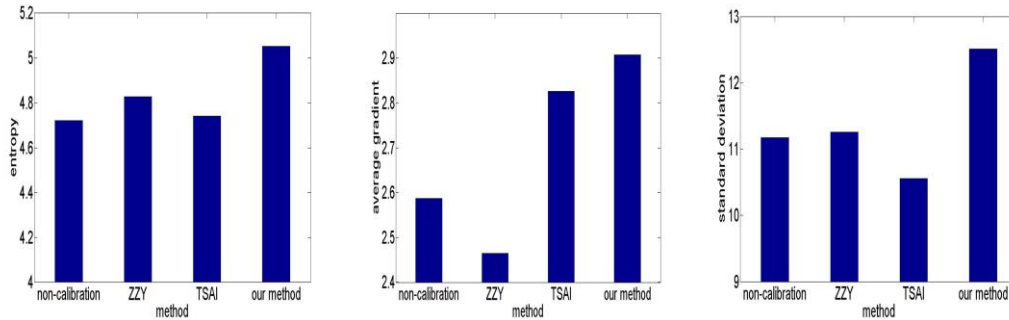


**Figure 14. The Performance Comparison of the Calibrated AOP Images**

From the AOP images of our calibration method and non-calibration, we can find that the entropy of AOP increased by 8%, the average gradient of AOP increased by 13% and the standard deviation increased by 12%. So our method is better and has certain advantages on the enriching target texture information when is applied to the underwater scene.

## 5. Conclusion

In this paper, we propose a method of calibration based on the radian of distorted curves in the checkboard, and we can calculate the coordinates of distortion center and calibration parameters independently. We choose the smallest radian of curves in X and Y direction respectively to calculate the two optical central line by iteration to get the distortion center and calibrate the region near the distortion center, then use sub regional strategy to continue the whole image reconstruction. After combining the distorted image, the reconstructed image and the distortion model, we obtain the calibration parameters to calibrate distorted images, and we obtain more edge contour information as a result. Experiments show that our method can calibrate the polarization image accurately, reduce the coupled error and calculate parameters independently. Moreover, the entropy of AOP can increase by 8%, the average gradient of AOP can increase by 13%, the standard deviation can increase by 12% and we can get more target texture information. This distortion correction method in this paper does not involve thin prism distortion, in future work, we need take it into account so that our method can be used in higher precision occasion. This method can significantly improve the quality of processed underwater image in many occasions, such as underwater target depth image acquisition, three-dimensional reconstruction of underwater target.

## Acknowledgment

This paper is partially supported by National Natural Science Foundation of China (No. 61263029, No. 61374019), a project funded by the priority academic program development of Jiangsu Higher Education Institutions(PAPD), and the Fundamental Research Funds for the Central Universities.

## References

- [1] W. C. Cox, B. L. Hughes and J. F. Muth, "A polarization shift-keying system for underwater optical communications", *Oceans, Mts/IEEE Biloxi-marine Technology for Our Future: Global & Local Challenges*. IEEE, (2009).
- [2] Y. Zhao, P. Gong and Q. Pan, "Object detection by spectropolarimetric imagery fusion", *Geoscience and Remote Sensing*, vol. 46, no. 10, (2008), pp. 3337-3345.
- [3] L. F. Meng and J. P. Kerekes, "An analytical model for optical polarimetric imaging systems", *Geoscience and Remote Sensing*, vol. 52, no. 10, (2014), pp. 6615-6626.
- [4] Y. Li and S. Wang, "Underwater polarization imaging technology", *Conference on Lasers & Electro Optics & the Pacific Rim Conference on Lasers & Electro-optics*. IEEE, (2009).
- [5] R. Y. Tsai, "A Versatile camera calibration technique for high-accuracy 3D machine vision metrology using off-the-shelf TV cameras and lenses", *IEEE Journal of Robotics and Automation*, vol. 3, no. 4, (1987), pp. 323-344.
- [6] Z. Y. Zhang, "A flexible new technique for camera calibration", *IEEE Transactions on Pattern Analysis and Machine Intelligence*, vol. 22, no. 11, (2000), pp. 1330-1334.
- [7] J. H. Won, T. Pany and B. Eissfeller, "Iterative maximum likelihood estimators for high-dynamic GNSS signal tracking", *Aerospace and Electronic Systems*, vol. 48, no. 4, (2012), pp. 2875-2893.
- [8] S. XU, X. X. SUN and X. LIU, "Geometry Method of camera self-calibration based on a rectangle", *Acta Optica Sinica*, vol. 34, (2014), pp. 233-246.
- [9] T. Rahman and N. Krouglicof, "An efficient camera calibration technique offering robustness and accuracy over a wide range of lens distortion", *Image Processing*, vol. 21, no. 2, (2012), pp. 626- 637.
- [10] R. Melo, J. P. Barreto and G. A. Falcao, "New solution for camera calibration and real-time image distortion correction in medical endoscopy—initial technical evaluation", *Biomedical Engineering*, vol. 59, no. 3, (2012), pp. 634- 644.
- [11] W. Wong, "Mathematical formulation and digital analysis in close range photogrammetric", *Photogrammetric Engineering and Remote Sensing*, vol. 41, no. 12, (1975), pp. 1355-1373.
- [12] S. Rhode, K. Usevich and I. Markovsky, "A recursive restricted total least-squares algorithm", *Signal Processing*, *IEEE Transactions on*, vol. 62, no. 21, (2014), pp. 5652 - 5662.
- [13] J. Wang, F. Shi and J. Zhang, "A new calibration model and method of camera lens distortion", *Intelligent Robots and Systems*, IEEE, (2006).
- [14] A. Franchois and C. Pichot, "Microwave imaging-complex permittivity reconstruction with a levenberg-marquardt method", *Antennas and Propagation*, vol. 45, no. 2, (1997), pp. 203-215.
- [15] J. Yang, Y. Yamaguchi and H. Yamada, "The characteristic polarization states and the equi-power curves", *Geoscience and Remote Sensing*, vol. 40, no. 2, (2002), pp. 305-313.